CrossMark

The Global Survey Method Applied to Ground-level Cosmic Ray Measurements

A. Belov[1] · E. Eroshenko[1] · V. Yanke[1] · V. Oleneva[1] ·
A. Abunin[1] · M. Abunina[1] · A. Papaioannou[2,3] ·
H. Mavromichalaki[2]

Abstract The global survey method (GSM) technique unites simultaneous ground-level observations of cosmic rays in different locations and allows us to obtain the main characteristics of cosmic-ray variations outside of the atmosphere and magnetosphere of Earth. This technique has been developed and applied in numerous studies over many years by the Institute of Terrestrial Magnetism, Ionosphere and Radiowave Propagation (IZMIRAN). We here describe the IZMIRAN version of the GSM in detail. With this technique, the hourly data of the world-wide neutron-monitor network from July 1957 until December 2016 were processed, and further processing is enabled upon the receipt of new data. The result is a database of homogeneous and continuous hourly characteristics of the density variations (an isotropic part of the intensity) and the 3D vector of the cosmic-ray anisotropy. It includes all of the effects that could be identified in galactic cosmic-ray variations that were caused by large-scale disturbances of the interplanetary medium in more than 50 years. These results in turn became the basis for a database on Forbush effects and interplanetary disturbances. This database allows correlating various space-environment parameters (the characteristics of the Sun, the solar wind, *et cetera*) with cosmic-ray parameters and studying their interrelations. We also present features of the coupling coefficients for different neutron monitors that enable us to make a connection from ground-level measurements to primary cosmic-ray variations outside the atmosphere and the magnetosphere. We discuss the strengths and weaknesses of the current version of the GSM as well as further possible developments and improvements. The method developed allows us to minimize the problems of the neutron-

✉ A. Papaioannou
atpapaio@astro.noa.gr

A. Belov
abelov@izmiran.ru

[1] Institute of Terrestrial Magnetism, Ionosphere and Radiowave Propagation by N.V. Pushkov RAS (IZMIRAN), Moscow Troitsk, Russia

[2] Nuclear and Particle Physics Department, Faculty of Physics, National and Kapodistrian University of Athens, 15784 Athens, Greece

[3] Institute for Astronomy, Astrophysics, Space Applications and Remote Sensing (IAASARS), National Observatory of Athens, I. Metaxa & Vas. Pavlou St., 15236, Penteli, Greece

monitor network, which are typical for experimental physics, and to considerably enhance its advantages.

1. Introduction

Ground–level detectors of cosmic rays (CR) have a number of advantages. They have no restrictions by weight, and therefore it is easy to construct them to cover a larger area; they are much cheaper than spacecraft detectors; it is easier to control and maintain them in working order, *etc*. The main problem of any ground-level detector, and in particular of neutron monitors (NMs), is that although they are created with the aim of studying variations in primary cosmic rays, they actually record their secondary products (Simpson, 2000).

The world-wide network of CR stations records secondary particles that are produced in the Earth's atmosphere when the primary CRs reach the atmosphere and interact with its molecules. In general, variations in the counting rate of a ground-based detector, for each detector denoted by i, can be written as

$$\delta_i = \left(\frac{\Delta N}{N_0} \right)^i = \delta_i^{\mathrm{EX}} + \delta_i^{\mathrm{AT}} + \delta_i^{\mathrm{MAG}} + \delta_i^{\mathrm{AP}} + \epsilon_i, \tag{1}$$

where:

– N_{0i} is the count rate of a neutron monitor during a reference time period (this period is the same for all NMs and is usually selected during quiet days).
– δ_i^{EX} are variations of extraterrestrial origin that depend on solar activity and the processes in the interplanetary environment.
– δ_i^{AT} are atmospheric variations that are related to the impact of the CR on the atmosphere above the surface of the detector.
– δ_i^{MAG} are CR variations of magnetospheric origin that are caused by the state of Earth's magnetosphere at the time of the measurements.
– δ_i^{AP} are variations due to the apparatus.
– ϵ_i is the term that includes variations that are not taken into account in the above terms, and constitute the occasional part of the variation.

Out of all of these components, variations that have an extraterrestrial origin are most interesting for the research of solar-terrestrial relations. However, in order to reliably select these variations from the NM data, it is necessary to be able to consider and identify variations of atmospheric and magnetospheric origin. This can be done with the help of response functions and coupling coefficients, which are described in more detail below.

The relationship between the observed counting rate and the rigidity-dependent flux of CRs at the top of the atmosphere is known as a response function. It combines the result of the particle transport within the atmosphere and the detection efficiency of an NM (Dorman, 1957, 1972; Dorman and Yanke, 1971a,b; Clem and Dorman, 2000). The coupling coefficient determines the contribution to the variation of the counting rate at a particular detector from the different components of the primary CR variation in the spherical expansion. The coupling coefficient depends on the referenced rigidity of the primary particles and on the rigidity dependence of the considered component. In practice, in order to determine the coupling coefficients, one needs to convolve the rigidity spectra of CRs with the response functions.

In order to properly take into account the influence of the atmospheric variations on the extraterrestrial effects on CRs, the theory of meteorological effects on CR was developed (Dorman, 1957, 1972, 2013; Dorman and Yanke, 1971a,b). In practice, variations in the count rate of NMs are particularly large due to changes in the mass of the air column above the detector. This is the main part of variations of atmospheric origin $[\delta_i^{\mathrm{AT}}]$, but fortunately since it closely correlates with the barometric pressure, it is as a rule excluded from the data – almost completely – at the first step of data processing (Dorman, 2013). Other types of atmospheric variations (*e.g.* dependence on the atmosphere temperature) are much smaller, and their influence can usually be neglected (see Dorman, 2013). However, it should be noted that in some cases, the effect of snow or wind may be significant on the measurements of several NM stations. Finally, variations due to the apparatus $[\delta_i^{\mathrm{AP}}]$ are usually automatically detected and excluded at the primary data-processing stage. Nonetheless, they sometimes remain in the raw data and have to be excluded during the process of preparing the data.

Cosmic-ray particles are already altered at the border of the atmosphere. They remain primary particles, but the magnetic field of the Earth cuts off a considerable portion of them and changes the trajectories of the remaining particles (McCracken, Rao, and Shea, 1962; McCracken *et al.*, 1965; Shea, Smart, and McCall, 1968; Dorman, Smirnov, and Tyasto, 1971; Bieber and Evenson, 1995). The most essential component, as concerns the accuracy of the determination of the extraterrestrial variations $[\delta_i^{\mathrm{EX}}]$, is the variation of magnetospheric origin $[\delta_i^{\mathrm{MAG}}]$ (Dorman, 2009). This is because during geomagnetic storms, δ_i^{MAG} can be large and distort the results obtained (especially at mid-latitude NM stations). For this reason, variations of magnetospheric origin $[\delta_i^{\mathrm{MAG}}]$ are included in several different versions of the global data-processing methods (Dvornikov, Sdobnov, and Sergeev, 1983; Belov *et al.*, 2005).

The necessity of obtaining global CR parameters beyond the magnetosphere, independent of the location of an observation point on Earth, led to the creation of special methods that use data from as many NMs as possible, distributed around the globe. We seek to identify and quantify the extraterrestrial variations. However, for this task, we have to be able to consider the influence of the atmosphere and magnetosphere.

Equation 1 captures the main types of variations in the count rate of NMs, but it remains simplistic. In particular, it should be supplemented by second-order variations that arise from the interaction of certain types of variations with the other terms. For example, extraterrestrial variations $[\delta_i^{\mathrm{EX}}]$ affect all other types, while magnetospheric variations $[\delta_i^{\mathrm{MAG}}]$ affect the atmospheric ones $[\delta_i^{\mathrm{AT}}]$. Since even the main variations are relatively small, second-order factors are substantially smaller and thus those are not taken into account separately; however, together with the statistical variations, they form part of the additional term ϵ_i.

One of the very first and successful realizations of a global method was created in Yakutsk (Krymsky *et al.*, 1966a,b, 1981; Altukhov, Krymsky, and Kuzmin, 1970) and was called the global survey method (GSM). At about the same time, Japanese researchers independently developed their own technique (Nagashima, 1971). Some time later, in the 1970s, a modification of the GSM was developed in the Institute of Terrestrial Magnetism, Ionosphere and Radiowave Propagation (IZMIRAN) (Belov *et al.*, 1973, 1974) and was applied to several events that were detected in October 1969 in the hourly data of the NM network. Then, the group of Irkutsk researchers developed their own version of a global spectrographic method (Sergeev, 1974; Dorman, 2009, 2013), which has more components and can be applied to more purposes than previous NM data-processing methods. It has been used successfully to define variations in the planetary distribution of geomagnetic cutoff rigidities and to calculate the second harmonic of the CR anisotropy in various events (Dvornikov, Sdobnov, and Sergeev, 1983; Richardson *et al.*, 2000; Dvornikov, Kravtsova, and Sdobnov,

2006; Lukovnikova, 2012). When the GSM is applied to NM data, it combines three techniques: i) the method of response functions, ii) trajectory calculations of a particle moving in the terrestrial magnetic field, and iii) expressing the variation of the CR intensity in terms of spherical harmonics. If the network of NMs were located outside of the atmosphere and the magnetosphere, the task (*i.e.* application of the GSM) would be reduced to the spherical harmonic analysis (third technique). In particular, the techniques are applied subsequently as follows:

– Calculation of response functions that transform the CR variations that are recorded at an observational point on Earth (*i.e.* NM) to the variations of the CR on the outer limit of the atmosphere, *i.e.* those that allow considering the interaction of the primary and secondary particles of various energy with the substance of the atmosphere (Dorman, 1957, 1972; Dorman and Yanke, 1971a,b; Clem and Dorman, 2000).
– The second component is the method of calculating particle trajectories in the terrestrial magnetic field. The terrestrial magnetosphere redirects incoming particles of various energies from their initial direction of motion (asymptotic) in near-Earth space and acts similarly to a spectrometer. The disturbances in the Earth's magnetic field can cause an essential change in the charged-particle trajectories in a magnetosphere even up to the point where the trajectories of particles that would be resolved in a quiet magnetosphere can become forbidden (Dorman, Smirnov, and Tyasto, 1971). Owing to changes in the Earth's magnetic field, the effective thresholds of the cutoff rigidity and the effective asymptotic directions for stations change as well. In order to consider the motion of the charged particles within the Earth's magnetosphere, cascade processes in the atmosphere and the detector properties, the coupling coefficients, and response functions for each station are used. This allows conversion from the variations in secondary CRs, observed on Earth, into the CR intensity in space, beyond the magnetosphere. The calculation methods for these coefficients and the computation results have been described in detail and are included in several works (McCracken, Rao, and Shea, 1962; McCracken *et al.*, 1965; Krymsky *et al.*, 1966a; Shea, Smart, and McCall, 1968; Altukhov, Krymsky, and Kuzmin, 1970; Nagashima, 1971; Nagashima *et al.*, 1989; Belov and Eroshenko, 1981; Yasue *et al.*, 1982; Kobelev *et al.*, 2013); ftp://cr0.izmiran.ru/GSM/CCn.
– The third part of the GSM is the spherical analysis (see, *e.g.*, Krymsky *et al.*, 1966a,b; Chirkov *et al.*, 1967; Nagashima, 1971; Belov *et al.*, 1973; Belov, 1980), which allows selecting spherical harmonics that are significant for a specific objective; for example, isotropic and anisotropic variations in the CR intensity outside the magnetosphere for any time intervals.

The history of GSM development in IZMIRAN has been long. The method has been changed and enhanced repeatedly. The most essential changes were made in the early 1990s and aimed at a simplified, but more reliable and convenient, technique for applications. With the help of this method, we have gradually processed the hourly data of the world-wide network of NMs, which covers the entire historical record of observations. Although the GSM has been available and intensively used for a long time (Belov *et al.*, 2005, 2014, 2015; Papaioannou *et al.*, 2009a,b, 2010; Papailiou *et al.*, 2012a,b, 2013), it has not been described in detail so far. We here intend to fill this gap and to provide a detailed description of the GSM formulation in the way it is constantly applied in IZMIRAN to calculate the main CR parameters and the CR intensity beyond the magnetosphere in various time intervals. This provides the possibility of studying various disturbances that are identified in the solar wind. Finally, we also discuss the advantages and the disadvantages of the method, and we point out how it might be improved.

Figure 1 Definition of the asymptotic directions λ and ψ for moving particles and geographic coordinates of the observation point [θ and φ] (adopted from McCracken, Rao, and Shea, 1962).
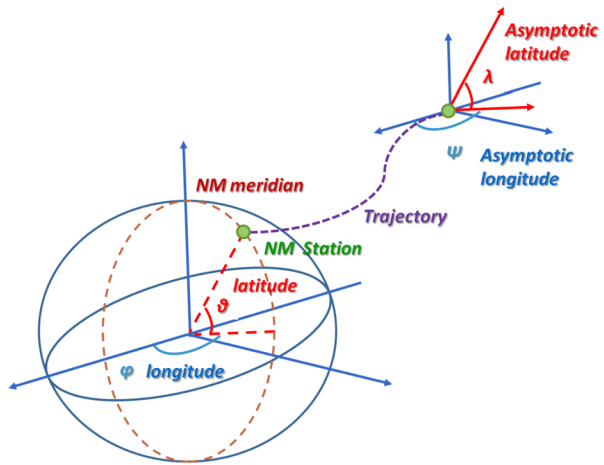
2. Essence of the Global Survey Method

The CR intensity, like any function, can be presented by the expansion formula in spherical harmonics (see Krymsky *et al.*, 1966a,b; Nagashima, 1971):

$$J(R, \theta, \varphi) = \sum_{n=0}^{\infty} \sum_{m=0}^{n} \left[\alpha_n^m \cos m\varphi + \beta_n^m \sin m\varphi \right] P_n^m (\sin \theta), \qquad (2)$$

where P_n^m are the conjunction Legendre functions, and θ and φ are the latitudinal and longitudinal asymptotic angles in the chosen coordinate system (in particular, it may be a geographical system), *the indices m and n refer to the particular term in the spherical harmonic series*. Figure 1 shows a schematic presentation of the angular characteristics of the moving particle beyond the magnetosphere (asymptotic directions) and near-Earth (geographic coordinate system).

In almost all cases, the CR variations at any observation point [i] may be presented as the sum of the zero-order and two first spherical harmonics of an expansion in Legendre polynomial (Krymsky *et al.*, 1981). In turn, the *count rate* variation for the i-station can be expressed through the coupling coefficients as

$$\delta_i = \delta_i^{\text{ex}} = \sum_{k=0}^{\infty} C_{ik}(\beta) A_k. \qquad (3)$$

Here A_k is the amplitude of the k-component of the anisotropy under fixed rigidity R_0, and C_{ik} is the coupling coefficient of the k-component in the i-point (station), which can be described by the following expression:

$$C_{ik} = \frac{\int_{R_c}^{\infty} \int_0^{2\pi} \int_0^{\frac{\pi}{2}} F_k(\theta_i(\lambda, \psi, R), \varphi_i(\lambda, \psi, R) f_k(R, \beta) W(R) N(\lambda, \psi) \sin \lambda \, d\lambda \, d\psi \, dR}{\int_{R_c}^{\infty} \int_0^{2\pi} \int_0^{\frac{\pi}{2}} W(R) N(\lambda, \psi) \sin \lambda \, d\lambda \, d\psi \, dR}, \qquad (4)$$

where:

– λ and ψ are the zenith and azimuthal angles of an incoming particle (asymptotic directions).

- θ and φ are the latitude and longitude of the point of observation in a geographic coordinate system.
- $W(R)$ is the response function of a detector.
- $N(\lambda, \psi)$ is the diagram of detector directions (*i.e.* the sensitivity of an NM to the particles arriving from various zenith and azimuthal angles).
- n – is the number of harmonics.
- k – is the component index in the spherical harmonic expansion.
- F_k and f_k – see below.

The derived coupling coefficients reveal the response of a CR detector to different components of the CR intensity expansion by the spherical harmonics.

Depending on how many harmonics are necessary, the number of coupling coefficients for each station will vary. For example, for the zero harmonic only one coupling coefficient ($k = 0$) is necessary; for the first harmonic, three coupling coefficients ($k = 1 - 3$), and for the second harmonic already five coupling coefficients are necessary for each station (Belov, 1980). For zero and first harmonics, we need four coupling coefficients.

In addition to the response functions, in the basis for calculating the coupling coefficients lie the asymptotic directions of arrival of the particles, which are represented in Equation 4 in terms of the function F_k. To each k (number of harmonics components) correspond various sub-integral angular functions $F_k(\theta_i(\lambda, \psi, R), \varphi_i(\lambda, \psi, R))$ that define a fraction of the particles incoming to this point in a particular corner (λ, ψ) from the possible asymptotic directions $F_k(\theta_i, \varphi_i)$,

$$
F_k\big(\theta_i(\lambda, \psi, R), \varphi_i(\lambda, \psi, R)\big) =
\begin{cases}
1, & k = 0, \\
\sin\theta, & k = 1, \\
\cos\theta\cos\varphi, & k = 2, \\
\cos\theta\sin\varphi, & k = 3, \\
3/2\sin\theta - 1/2, & k = 4, \\
\sqrt{3}\cos\theta\sin\theta\sin\varphi, & k = 5, \\
\sqrt{3}\cos\theta\sin\theta\cos\varphi, & k = 6, \\
\sqrt{3}/2\cos^2\theta\sin 2\varphi, & k = 7, \\
\sqrt{3}/2\cos^2\theta\cos 2\varphi, & k = 8, \\
\cdots.
\end{cases}
\tag{5}
$$

To calculate the coupling coefficients, it is also necessary to define a type of a spectral function $f_k(R, \beta)$, where β is the vector of a spectral characteristic: in the case of power spectra, this is a spectral index, and in a more complicate case this is a set of parameters. Since the spectral function is different for various harmonics, the index n is the number of harmonics for which we should choose a spectral function. One version of using this function was considered by Belov and Eroshenko (1981). To derive a best-fit set of the parameters that define the primary CR variations, the least-squares method (LSM) is commonly used, which minimizes the following expression for each of the n stations:

$$
D = \frac{\sum_{i=1}^{n} g_i [\delta_i - \sum_{k=0}^{m-1} \alpha_k C_{ik}(\beta)]^2}{n - m}.
\tag{6}
$$

We note that the indices m and n do not refer to the particular term in the spherical harmonic series. Here n stands for the number of stations (*i.e.* NMs), and m is the number of unknown parameters (*e.g.* $m = 5$, if limited to zero and the first harmonics).

3. Practical Use of the Global Survey Method

We have described that it is enough to use the first three harmonics of the spherical expansion (zero, first, and second order) for almost all modulation effects, and it is often enough to use only the first two (zero and first order) for a wide range of tasks.

When limited to the zero- and first-order harmonics (isotropic part and three components of the first anisotropy harmonics), the CR variations expected at Earth can be expressed as a system of equations for each observation point i at height h with the rigidity of the geomagnetic cutoff of R_c at time t as

$$\delta_i = A_0 C_{0i}(\gamma) + C_{xi} A_x + C_{yi} A_y + C_{zi} A_z. \tag{7}$$

Here, $A_0 C_{0i}(\gamma)$ is the contribution of the zero harmonic to CR variations (isotropic part): A_0 is the amplitude of the zero harmonic; γ is the spectral index of the variation, which particularly may be defined as a power law in rigidity; A_x, A_y, and A_z are the three components of the first harmonic of the CR anisotropy in Cartesian coordinates; and C_{xi}, C_{yi}, C_{zi} are the corresponding coupling coefficients for each of the components (Belov, 1980; Asipenka *et al.*, 2009).

The system of Equations 7 is solved by minimizing the sum of squares of the residuals of unknown parameters that characterize spectrum variations in primary CR intensity [A_0 and γ], and also of the anisotropy vector components [A_x, A_y, and A_z]. These characteristics are derived in the geographical coordinate system connected with a zero meridian. For a transition to the coordinate system connected with the Sun, it is necessary to express ϕ_h in terms of the solar day $2\pi/24(T + 1/2)$, where T is the time in hours. The coupling coefficients of the zero harmonic are relatively simple to calculate as

$$C_{0i}(\gamma) = \int_{R_{ci}}^{R_u} R^{-\gamma} W_i(R_{ci}, h, R) \, \mathrm{d}R, \tag{8}$$

where $W_i(R_{ci}, h, R)$ are the response functions for the primary and secondary CR variations for a device i, located at a level h_i at a point with a cutoff rigidity R_c.

It is very computationally expensive to calculate the coupling coefficients for the first and higher harmonics because not only does the interaction of the CR with the Earth's atmosphere (which involves the response functions $W^i(R_{ci}, h, R)$) need to be considered, but also the influence on the CRs of the Earth's magnetosphere, for which the directions of the CR motion at various energies outside the magnetosphere (asymptotic) are required. Asymptotic directions for different stations of the world-wide network were calculated in various works (see, *e.g.*, McCracken *et al.*, 1965; Shea *et al.*, 1968). We make use of the coupling coefficients calculated by a group of Japanese authors for the minimum and maximum solar activity. Yasue *et al.* (1982) presented tables of the coupling coefficients for many stations. The coefficients were calculated for various indices of a spectrum γ ($-1.5, -1.0, -0.5, 0.0, 0.5,$ and 1.0) and different upper thresholds of the rigidity R_u, above which the anisotropy disappears (30, 50, 100, 200, 500, and 1000 GV). All of these coefficients were entered into the database of the working GSM program and are used during the calculations. Table 1 provides such an example for the Moscow neutron monitor station. Coupling coefficients calculated for all stations of the worldwide network may be retrieved at the following URL: spaceweather.izmiran.ru/rus/cc3.html.

The response functions and the coupling coefficients for the isotropic part of the CR were computed in each calculation for the respective number of stations and the chosen time period. During the realization of the GSM, we often use stations for which the coupling

Table 1   Example of coupling coefficients for the Moscow station for $\gamma = -1.5$ and $\gamma = 0.0$.

γ	R_u	$C00$	$C10$	$C20$	$C11$	$\phi11$	$C21$	$\phi21$	$C22$	$\phi22$
−1.5	30	0.914	−0.0093	−0.4181	0.685	72.37	0.0864	−35.19	0.432	136.35
−1.5	50	0.927	−0.0015	−0.4167	0.692	71.92	0.0898	−29.65	0.435	135.72
−1.5	70	0.93	0.001	−0.4158	0.694	71.8	0.0911	−28.37	0.435	135.58
−1.5	80	0.931	0.0015	−0.4155	0.694	71.77	0.0914	−28.1	0.435	135.56
−1.5	100	0.932	0.0022	−0.4151	0.695	71.74	0.0919	−27.8	0.435	135.52
−1.5	150	0.933	0.0029	−0.4148	0.695	71.7	0.0923	−27.53	0.435	135.49
−1.5	200	0.933	0.0031	−0.4147	0.695	71.69	0.0925	−27.45	0.435	135.49
−1.5	300	0.933	0.0033	−0.4146	0.695	71.68	0.0926	−27.4	0.435	135.48
−1.5	500	0.933	0.0033	−0.4145	0.695	71.68	0.0926	−27.38	0.435	135.48
−1.5	1000	0.933	0.0034	−0.4145	0.695	71.68	0.0927	−27.37	0.435	135.48
0	30	0.63	0.0787	−0.2502	0.549	55.9	0.132	32.79	0.396	108.51
0	50	0.724	0.137	−0.2383	0.613	53.83	0.199	33.71	0.429	105.63
0	70	0.773	0.171	−0.225	0.64	52.67	0.232	32.84	0.439	104.19
0	80	0.789	0.183	−0.2193	0.649	52.25	0.244	32.39	0.442	103.7
0	100	0.815	0.202	−0.21	0.661	51.59	0.26	31.6	0.445	102.96
0	150	0.853	0.231	−0.1953	0.678	50.55	0.285	30.21	0.448	101.84
0	200	0.876	0.248	−0.1865	0.687	49.92	0.299	29.31	0.449	101.2
0	300	0.902	0.267	−0.1761	0.698	49.17	0.314	28.21	0.449	100.46
0	500	0.927	0.287	−0.1658	0.707	48.43	0.329	27.11	0.449	99.75
0	1000	0.951	0.305	−0.1559	0.716	47.7	0.344	26.05	0.449	99.07

coefficients in the tables of Yasue *et al.* (1982) are lacking. In these cases, we interpolate the available coupling coefficients.

We note that $C00$ is the coupling coefficient for the isotropic component of the CR, $C10$ is the coefficient for the north–south component, and $C11$ and $\phi11$ are the coupling coefficient and phase shift of the solar-diurnal component of the first harmonic of the CR anisotropy in the polar coordinate system; $C20$ is the coupling coefficient for the second zonal component; and $C21$, $C22$, $\phi21$, and $\phi22$ are the coupling coefficients and phase shift for the equatorial component of the second harmonic of the CR anisotropy.

For the transition to a Cartesian coordinate system, it is necessary to carry out the following transformations for each station taking into account its longitude ϕ_s:

$$\begin{cases} C_{xi} = C_{11} \cos(\phi_s + \phi_{11}), \\ C_{yi} = C_{11} \sin(\phi_s + \phi_{11}), \\ C_{zi} = C_{10}, \end{cases} \tag{9}$$

where for the first harmonic the amplitude [$C11$] and the phase [$\phi11$] define the particle shift in the magnetosphere. Although the coupling coefficients for the zero harmonic are also presented in the tables, we perform independent calculations of $C00$ according to Equation 8 for any observation point using the response functions of the CR intensity at the boundary of the atmosphere and at the observation point (Dorman, 1957; Dorman *et al.*, 1970; Clem and Dorman, 2000):

$$W(R) = \alpha(k - 1) \exp\left(-\alpha R^{-(k-1)}\right) R^{-k}. \tag{10}$$

Figure 2 Coupling coefficients for the zero harmonic calculated based on Equation 8 for $\gamma = 0.5$. *Black circles* refer to NMs at sea level, and *blue circles* represent NMs on mountains.
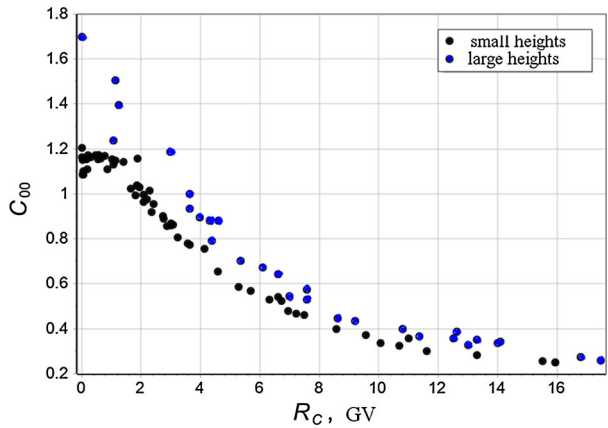
Aleksanyan *et al.* (1979) derived an approximation of the altitudinal variation of the parameters α and k, which can be presented by the following expression (h in bars):

– for the minimum of solar activity (1965),

$$\begin{cases} \ln \alpha = 1.84 + 0.094h - 0.09 \exp[-11h], \\ k = 2.40 - 0.56h + 0.24 \exp[-8.8h]. \end{cases} \tag{11}$$

– For the maximum of the solar activity (1969),

$$\begin{cases} \ln \alpha = 1.93 + 0.150h - 0.18 \exp[-10h], \\ k = 2.32 - 0.49h + 0.18 \exp[-9.5h]. \end{cases} \tag{12}$$

As we show below, up to a level of 300 mbar, the dependence on the height of the parameters that we focus on here has an almost linear variation.

3.1. Isotropic Part of the CR – Zero Harmonic in Spherical Expansion

We calculate the response functions and the coupling coefficients for the isotropic part of CR at each account depending on the choice of stations and the processing period.

Figure 2 shows the coupling coefficients for the zero harmonic for all CR stations of the existing world-wide network and the cutoff rigidities range from 0 to 16 GV for $\gamma = 0.5$.

The behavior of the coupling coefficient for the isotropic component ($C00$) reflects the ability of each station to respond to the CR modulation. Additional information about the contribution of each station into the recording of the isotropic part of the CRs is also provided in Figure 3, where the distribution of the expected isotropic variation in the currently operational NMs is presented for two power-rigidity spectra of primary CR variations with indices $\gamma = 1.0$ (left) and $\gamma = 0.5$ (right). The NM stations that have a higher-than-average ability in this respect (*i.e.* respond to the modulation of CRs) within the range of cut-off rigidities R_c from 0.5 to 3.5 GV are Mount Washington (MTWS), Calgary (CALG), and Climax (CLMX), while the lowest response to the CR modulation is reported at the recently opened station in Thailand (Princess Sirindhorn: PRSI) (Shea *et al.*, 1987). Four-character names of NM stations are used by the NM scientific community according to a format developed by Shea and co-authors to standardize the list of stations in the study of GLE events.

Figure 3 Distribution of the expected isotropic CR variation on the currently operational NMs for two power-rigidity spectra $R^{-\gamma}$ of the primary CR variation for indexes $\gamma = 1.0$ (*left*) and $\gamma = 0.5$ (*right*).
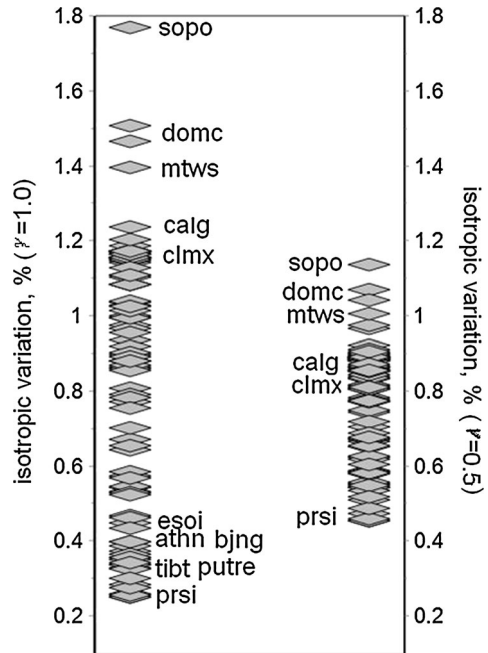

The largest difference in the variations is observed between stations that have the highest and lowest $C00$ coefficients (stations at high latitude and near the Equator, respectively). These stations are most valuable for the definition of an inclination and the form of the rigidity spectrum of a variation. Stations with the lowest sensitivity to the CR modulation are no less important than stations with the maximal sensitivity, however.

While at the top end of the $C00$ coefficients, the situation is favorable and the existing NM network uses the capabilities of the ground-level observations to full extent, this is not the case at the lower end. It is known (Smart, 1997) that there are points on the Earth (in Southeast Asia and the Indian Ocean) where the rigidity of the geomagnetic cutoff can reach 17.6 GV. For the stations that were operational until recently, the highest R_c was 13.3 GV (Haleakala: HLEA) and if only the NM stations close to sea level were to be selected, then the highest R_c would be about 9.6 GV (Bejing: BJNG). The new Princess Sirindhorn station, which recently opened, with the highest rigidities of the geomagnetic cutoff ($R_c \approx 16.8$ GV) only partially solves this problem. In addition, this is a mountain station, and in mountains, the variation of CR is larger. It is even more important that it is difficult to model mountain variations, however.

The rigidity spectrum of the CR variation has a slope that can be determined by directly deriving the dependence of an observed variation on R_c. This is currently only possible for rigidities between $2 - 9.5$ GV. Thus, the network of NMs that is available today uses only half of the terrestrial range of cutoff rigidities. For the NM stations operated in earlier times, such as Kodaikanal ($R_c \approx 17.5$ GV), Lae, and Ahmedabad, the isotropic variation at $\gamma = 1.0$ would not be 0.35% as at the Haleakala station, but $0.25 - 0.26$%. The minimum possible variation under these conditions for a sea-level station would be 0.22%. The network of NMs may still be altered such that the range of a reliable definition for the spectrum of a CR variation according to NM data is significantly extended, and the accuracy of this definition will significantly increase.

Figure 4 Dependence of the coupling coefficients of the first harmonic of the CR anisotropy on the cutoff rigidity [R_c] at the spectrum ($\gamma = 0.5$) up to an upper rigidity of 100 GV. (**a**) $C10$: coefficient of the north–south component, (**b**) $C11$: coefficient of the solar diurnal variation, and (**c**) $\phi11$: effective magnetospheric shift of the phase of the solar-diurnal variation. Data are given for NMs at sea level (*circles*) and for NMs at high altitudes (*triangles*).
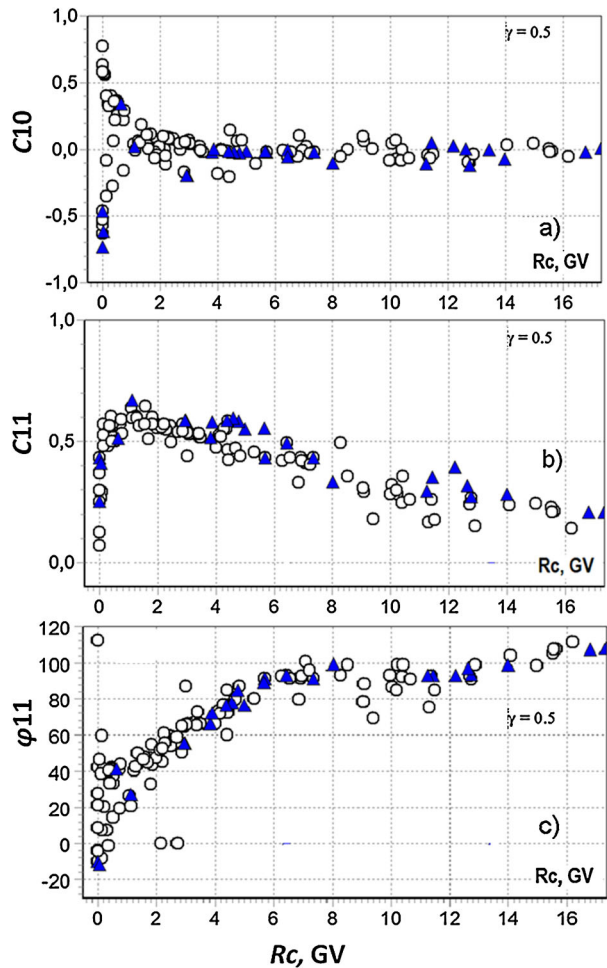
3.2. The First Harmonic of the CR Anisotropy

Panels a–c of Figure 4 show the behavior of the coupling coefficients for different components of the first harmonic of the CR anisotropy as a function of the cutoff rigidity [R_c] at the observation point.

Analyzing the rigidity dependence of the coupling coefficients helps us to understand the role of a particular station in registering the different components of the CR variations and in determining the characteristics of these components (Moraal, Belov, and Clem, 2000).

Figure 5 shows the distribution of the expected contribution from the north–south (left) and the equatorial (solar-diurnal, right) components of the CR anisotropy in the recorded CR variation of the NMs that are currently operational.

Most NMs of the world-wide network collect particles from the equatorial zone, and only a few stations near the poles are able to "see" particles incoming from high asymptotic latitudes. These latter stations play a major role in determining the north–south anisotropy. In the northern hemisphere, these stations are Thule (THUL) and Barentsburg (BRBG), and the stations in the southern hemisphere are McMurdo (MCMU) and Terre Adelie (TERA).

Figure 5 Distribution of the
expected contribution from the
north–south (*left*) and the
equatorial (solar-diurnal, *right*)
components of the CR anisotropy
in the count-rate variation of the
NMs that are currently
operational.
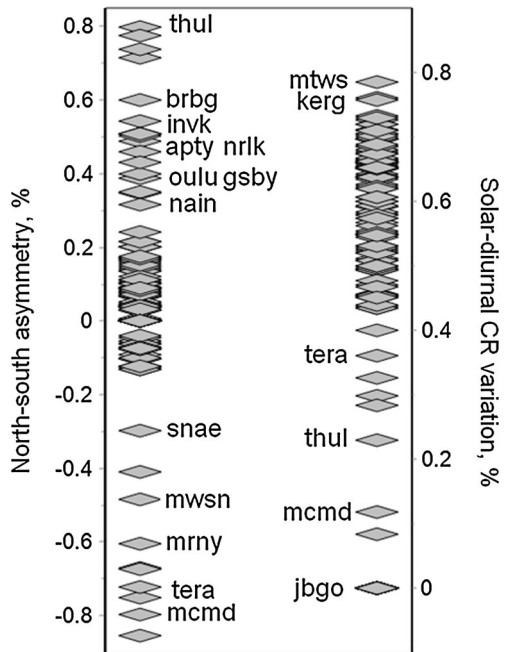
The pair of stations Thule and McMurdo is good. They present the highest response and a symmetric, equal contribution in the N–S anisotropy as well as on the variations of the CR density, but they hardly respond to the equatorial anisotropy and the geomagnetic CR variations. Therefore it is quite reasonable to use the half-difference of the variations at these stations to estimate the amplitude of the N–S anisotropy, and the half-sum – instead of the isotropic variation, as was done, for example, by Pomerantz and Duggal (1972). However, the limited number of stations with high coupling coefficients $C10$ for the N–S component makes this selection challenging and thus not always reliable. This means that variations of atmospheric or instrumental origin can be misunderstood as changes in the N–S anisotropy. The station at Thule had a suitable substitute in the Alert station. It is a great loss that valuable NM stations such as Resolute (in the North of Canada), Vostok, Wilkes, and Syowa (in Antarctica) are currently closed. On the other hand, the recent Russian station Barentsburg (BRBG) is closest to the station Thule and can compensate for it to a certain extent. Historical decisions and significant changes during recent years were made at the station McMurdo (MCMU). In late 2014, one six-tube section of the NM at MCMU was dismantled for shipment to the South Korean station at Jang Bogo (Jung *et al.*, 2016), approximately 374 km northeast of MCMU. This first section was installed and put into operation in December 2015. In the period from December 2015 to January 2017, the two partial stations operated in parallel and overlapped very well. The Jang Bogo station is now operating with five counters and has been normalized to the full 18-counter McMurdo monitor. In January 2017, the remaining two MCMU sections were dismantled and shipped to Jang Bogo. Full operation of the JBGO monitor is expected to begin in late 2017 or early 2018 (Jung *et al.*, 2016).

Today, Jang Bogo is still the only polar station in the southern hemisphere. The other Antarctic stations near the geographical pole (Dome C, the South Pole, Terra Adelie, Sanae, and Mirny) cannot be considered as polar for CRs because of their viewing directions: they
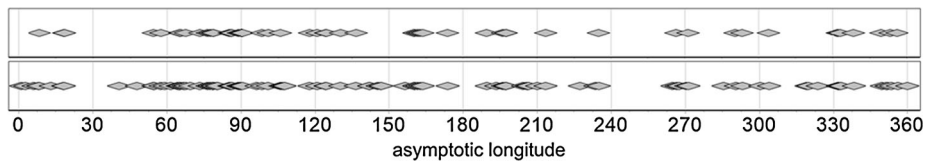
Figure 6 Distribution of the existing (*upper panel*) NMs and all stations that ever existed (*lower panel*) with respect to the asymptotic longitudes.

have a much stronger solar-diurnal variation and very low coupling coefficients for N–S anisotropy.

Stations with latitude of about 50° and a cutoff rigidity of about 1 GV (Calgary, Kerguelen) have the highest response to the solar-diurnal modulation [$C11$]. However, there are no clear leading stations here since almost all NM stations of the worldwide network are able to observe the solar-diurnal variation, and all together provide unique information about the angular distribution of the CRs. Figure 6 shows the values $\phi + \phi_1^1$ (ϕ – station longitude, ϕ_1^1 – drift angle of the particles in the Earth's magnetic field), characterizing the effective position of the station in recording the first harmonic of the anisotropy (asymptotic longitude) for all existing (top panel) and for all stations that ever existed (the lower panel). There is a certain distribution of stations around the globe that shows the geography of the distribution of water, land, and places of scientific research. The longitude range corresponding to the Pacific and Atlantic Oceans is particularly poorly covered by NMs.

Figures $4-6$ are plotted for a spectrum $\gamma = 0.5$ up to an upper rigidity of 100 GV. The distribution of the amplitudes and phases of the solar-diurnal variation can significantly change for another rigidity spectrum. These changes are small at high-latitude stations, which have the highest sensitivity to the solar-diurnal anisotropy, but these changes are much stronger at medium- and low-latitude stations since their acceptance cone is extended in longitude (Yasue *et al.*, 1982). These medium- and low-latitude ($R_c > 3.5$ GV) stations are particularly important for the determination of the anisotropy rigidity spectrum. A simple comparison of the daily waves in the behavior of CRs observed at two such stations is sometimes sufficient to estimate the characteristics of the spectrum, while all NM stations situated at the high-latitude ring cannot provide useful input for this.

4. Implementation of the GSM

Our model has no parameters that can be determined by only one station; therefore in practice we did not select the most complicated model for GSM, but we instead used a reasonable selection of stations. To determine the extraterrestrial variations of the CR, the coupling coefficients for the first harmonic were chosen at $\gamma = 0.0$ and the upper rigidity was $R_u = 100$ GV (*i.e.* with a flat spectrum of variations) in the GSM implementation. This simplification is quite acceptable, because the CR anisotropy does not strongly depend on the particle rigidity in quiet and quasi-stable periods (*e.g.* Krymsky *et al.*, 1981). In the model, the spectral index for the isotropic part is included as a variable that is estimated when the system of Equations 7 is solved, and correspondingly the coupling coefficients are used for its different values.

For the calculations, data are imported, corrected for atmospheric pressure, and checked for drifts and occasional spikes. In addition, we use the double recalculation to reject occasional spikes in data. Unlike other options of the GSM calculation of the GCR parameters, we use the sequence of steps described below.

4.1. Determining the Equatorial Component of the First Harmonic of the CR Anisotropy Based on Data of High-latitude Stations

For this task only high-latitude stations at sea level ($R_c < 3$ GV, $h > 800$ mb) are selected from the general table. Then the system of Equations 7 is solved for the parameters of both the isotropic and the anisotropic parts of the CR. Since the system is nonlinear and poorly conditioned, one way of solving this is by its linearization, applying the method of singular expansion (single value decomposition: SVD) (Forsythe, Malcolm, and Mouler, 1980). Moreover, we interpolated (spline approximation) the coupling coefficients for the intermediate values of γ and R_u to find the minimum dispersion to determine the GCR parameters. As a result, the required parameters of the GCR are obtained for each hour. Since the computations are carried out according to the full model (Equation 7) in the first stage: A_x, A_y, and A_z are the characteristics of the first harmonic of the CR anisotropy and A_0 and γ for the isotropic component of the CR are obtained. For the calculations, the count-rate variations relative to a base period $(N_i - N_0)/N_0$ are used instead of its absolute values. The choice of the base period (usually a day, the same for all stations) is important. The counting rate of each specific device is defined by a number of factors that are difficult to specify. At the same time, the uniformity of the sizes $[N_0]$ is also violated during disturbed periods because of magnetospheric and extraterrestrial variations. This leads to a false diurnal rotation of the phase of the equatorial component of the first harmonic of the CR anisotropy, especially if the period under consideration is far from the base period. To avoid this effect, we have to change the base period several times (three to seven times *per* month). This procedure does not affect the values of A_x and A_y components, but the behavior of A_0 and A_z components becomes multistage, which makes these parameters unsuitable for the analysis. They are determined in the second step of the GSM program.

4.2. Determining the Isotropic Component and the North–South Component of the First Harmonic of the CR Anisotropy

The complete list includes all of the stations for which the coupling coefficients $C00$ ($R_c < 17$ GV, $h > 600$ mb) were calculated. On the basis of the results for (A_x and A_y) obtained in the first step, and with the calculated coupling coefficients, the equatorial component of the first harmonic of the CR anisotropy is extracted from the data of each station with the equation

$$\delta_i^* = \delta_i - C_{xi} A_x - C_{yi} A_y, \tag{13}$$

where δ_i is the variation of the current count rate for the i NM, and δ_i^* is the count-rate variation corrected for solar diurnal anisotropy; C_x and C_y are the coupling coefficients for the equatorial component of the first harmonic of the CR anisotropy.

The data after the correction for the equatorial anisotropy practically include the response to the isotropic part of the primary CR and to the north–south component of the first harmonic of the CR anisotropy:

$$\delta_i^* = A_0 C_{0i}(\gamma) + C_{zi} A_z. \tag{14}$$

As a result, the system is solved with respect to parameters A_0, γ, and A_z by applying the least-squares method to the set of Equations 14. The evolving, larger number of stations clearly increases the accuracy of the received results considerably.

4.3. Opportunities for Improving the Global Survey Method

While working with GSM, a number of opportunities for its improvement and the more optimal usage of the method were identified. In particular, these are listed below:

  i) Specification of the model rigidity dependence for the isotropic part of the CR variation.
 ii) Replacement of the power-law spectral function with more complicated ones that have to affect, first of all, a research of the larger (with respect to duration and amplitude) Forbush decreases (FD).
iii) Introducing the second harmonic of the CR anisotropy in the model of variations.
 iv) Accounting for the magnetospheric variations.
  v) Introducing an optimal choice of the base period.
 vi) Definition of the rigidity dependence of the CR anisotropy and/or the accounting for its changes (this is essential at larger anisotropy).
vii) Accounting for changes of the response functions (and, as consequence, of the coupling coefficients) in time.
viii) Improvement of the quality of the incoming data.
 ix) Specification of the barometric coefficients and recalculating of the corresponding corrections.
  x) Adding, along with the NM data, measurements from other detectors, first of all, from muon telescopes that have the same inclination but different directions. It is easier to add variation differences from telescopes of the same type that have the same inclination.

5. Advantages of the Global Survey Method Compared to the Usage of the Data from a Single Cosmic Ray Station

Data from a single NM cannot provide a clear idea about the whole angular distribution of the CRs. To obtain the most complete information about the distribution of CRs outside the magnetosphere, it is necessary to have many detectors that are sufficiently evenly located on the globe. If the distribution of CRs is isotropic, we can estimate the isotropic component of the CR intensity when we know the coupling coefficients for an observation point with even a single station, although with a low accuracy. To define the CR anisotropy, however, one device (*i.e.* NM) is no longer sufficient: the first spherical harmonic requires at least four NMs; for the second harmonic we need at least even nine devices (Krymsky *et al.*, 1966b, 1981).

A large fraction of research on CR variations was based on data from one or sometimes several detectors (*i.e.* NMs). This is also the case today, especially for studies of Forbush effects (FEs). Therefore, in this part we discuss the problems arising in such works and show that the usage of GSM can offer solutions to these problems or can at least essentially reduce their negative impact.

We explained above that the world-wide network of CR stations consists of the separate detectors (first of all, NMs) at different locations around the globe that collect particles in particular cones of the asymptotic directions (a reception cone). In GSM, all stations of the network are used as a uniform multichannel device where each channel (station) provides information in a certain cone of the asymptotic directions, and all channels cover the entire celestial sphere. The many channels of such a device provide reliability and the continuity of

Figure 7 Count-rate variations at the Moscow NM (*blue line*) and the variations of CR density *A*0 obtained by the GSM for 10 GV particles (*brown line*) from 07–11 May 2016. The start time of the FE is depicted with a *magenta triangle*.
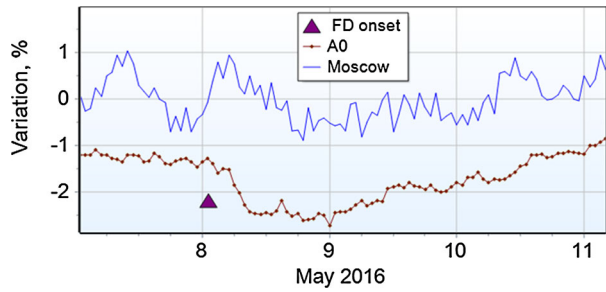

measurements. In comparison with the separate CR stations, the statistical accuracy of the network increases considerably and the influence of hardware effects decreases significantly. For example, the separate supermonitor provides a statistical accuracy of $0.1-0.2$ % h^{-1}, while the complete network of stations provides an accuracy of ≈ 0.05 % h^{-1}. However, it is even more important that the GSM allows determination of the density (the isotropic part of the intensity) and the anisotropy of galactic CRs outside the magnetosphere in each hour and separates one from another. The count rate of one NM contains both the isotropic part of the intensity and the anisotropy of CRs, which characterizes a small part of space, within the limits imposed by the asymptotic reception cones of this detector. Even assuming a constant anisotropy, its contribution to the count rate will constantly change because of the detector corotation with the Earth that creates a solar diurnal wave. Therefore, at different NMs, the effects of CRs will differ, for example the FE will have a different development and the characteristics of the FE obtained from the data of one NM will depend on the characteristics of this particular detector.

The separation of the CR density variations compared to the amplitude of the CR anisotropy is very problematic. We review specific examples. A period of five consequent days from 07–11 May 2016 is presented in Figure 7. This figure illustrates the results of the GSM for a small FE associated with a considerable coronal hole. Figure 7 captures at the beginning of the FE the area of interaction of a high-speed stream that approached Earth. In the variations of the CR density [*A*0] – obtained from the GSM – the FE is clearly visible, but this is not the case when inspecting the data of the Moscow NM station. Even when knowing the FE time (*e.g.* onset and duration), it is difficult to see the FE signs in the count rate of a single NM station. This is because the FE is distorted, first of all, by the daily wave created by the CR anisotropy here. We have chosen the Moscow NM station because this NM is rather typical for the sensitivity to the anisotropy of CRs, and owing to its 24 NM counters it has one of the best statistical accuracies of the NMs operating near sea level.

Figure 7 illustrates a rather common situation where it is not possible to identify FEs with a small amplitude using the data of a single NM. As is seen, this is valid for FEs with an amplitude $\approx 1\%$. At the same time, the output of the GSM makes it possible to reliably identify FEs with an amplitude of $0.3-0.5\%$. Such small (in magnitude) FEs are important, since they are often the response of CRs to powerful solar events and large interplanetary disturbances. Moreover, the absence (full or partial) of these small FEs significantly limits their usage in statistical studies.

Admittedly, large FEs can be identified in the recording of one NM, but how reliable will this isolated identification be? In Figure 8 we present a time period at the beginning of August 2016. A considerable FE of about 3% was observed. This FE is clearly visible, not only in the *A*0 density variations retrieved by the GSM, but also in the counting rate of the Moscow NM. However, it becomes obvious that it is difficult to estimate the FE amplitude

Figure 8 Count-rate variations at the Moscow NM (*blue line*) and the variations of CR density *A*0 obtained by the GSM for 10 GV particles (*brown line*) from 01 – 05 August 2016. The start time of the FE is depicted with a *magenta triangle*.
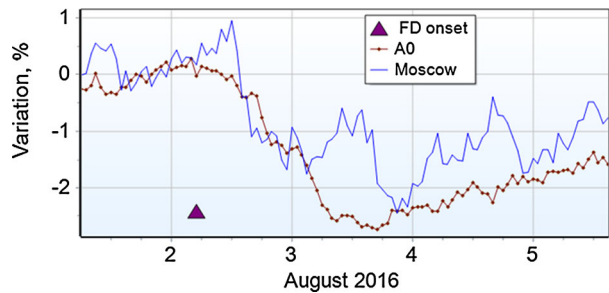
precisely and to define the FE onset or the time of the FE minimum based on the count rates of a single NM.

It is possible to try to correct the data for the influence of the anisotropy of CRs by smoothing or averaging the data *per* day (Lockwood, 1990; Alania, Szabelski, and Wawrzynczak, 2003). While attempting to average out the influence of the CR anisotropy, the effect significantly decreases (although it is not possible to correct for this influence completely), but other problems appear: in particular, the size of the actual effect is underestimated, which is in turn controlled by the duration of the FE. For example, when an FE lasts less than a day, the averaging can reduce the effect by a factor of two – three.

The event on 18 September 1959, in which the FE developed within one day, is presented in Figure 9a. In the data of one NM station, the daily wave that disappears in the behavior of the CR density obtained by the GSM is clearly visible. As a result, the data processing by means of the GSM resulted in an FE size of $\approx 8.8\%$, while based on the daily averaging of the MTWS NM data, it was only $\approx 3.8\%$. Thus, the observed effect on this station was underestimated by more than a factor of 2. A similar situation is observed for the study of the event on 07 May 1960 (see Figure 9b). The size of the FE when we apply the GSM was $\approx 10.1\%$, and based on the daily averaging data, it was $\approx 3.9\%$. In this case, the observed effect at the station was underestimated by more than a factor of 2.5.

This shows that studying short-duration FEs becomes a non-trivial task when data of a single NM station are used, even when the effect is more extended. Daily averaging cannot and should not be considered as a completely negative factor, however. When hourly data of a separate NM are used, then large distortions in the corresponding effects are inherited through the daily GCR variation.

Underestimating the size of the effects is not the only problem arising with daily averaging. Using such averaged data, we cannot study the CR anisotropy, details of the FD profile, and the internal structure of the interplanetary disturbance creating the FE. Moreover, averaged daily NM data are not proper for detailed studies of FEs and can only be recommended for research investigations that use data with low statistical accuracy.

It is possible to present several advantages of the GSM in greater detail, compared to using the individual CR stations. One such advantage is the measurement continuity. When using the GSM, if one NM fails, we lose only one channel (*i.e.* data on one direction). At the same time, data on other directions are collected reliably, and as a result, the data quality remains the same, in practice. If effects are investigated with data of only a single NM, however, then it is highly possible that all data are lost if that one NM fails.

Another limitation in using a single NM is the various artifacts that have been reported. They are detected as a change in CR density that is not associated with extraterrestrial variations. For example, accumulated snow on the roof of a building that hosts an NM can produce these artificial variations (Korotkov *et al.*, 2011, 2013).
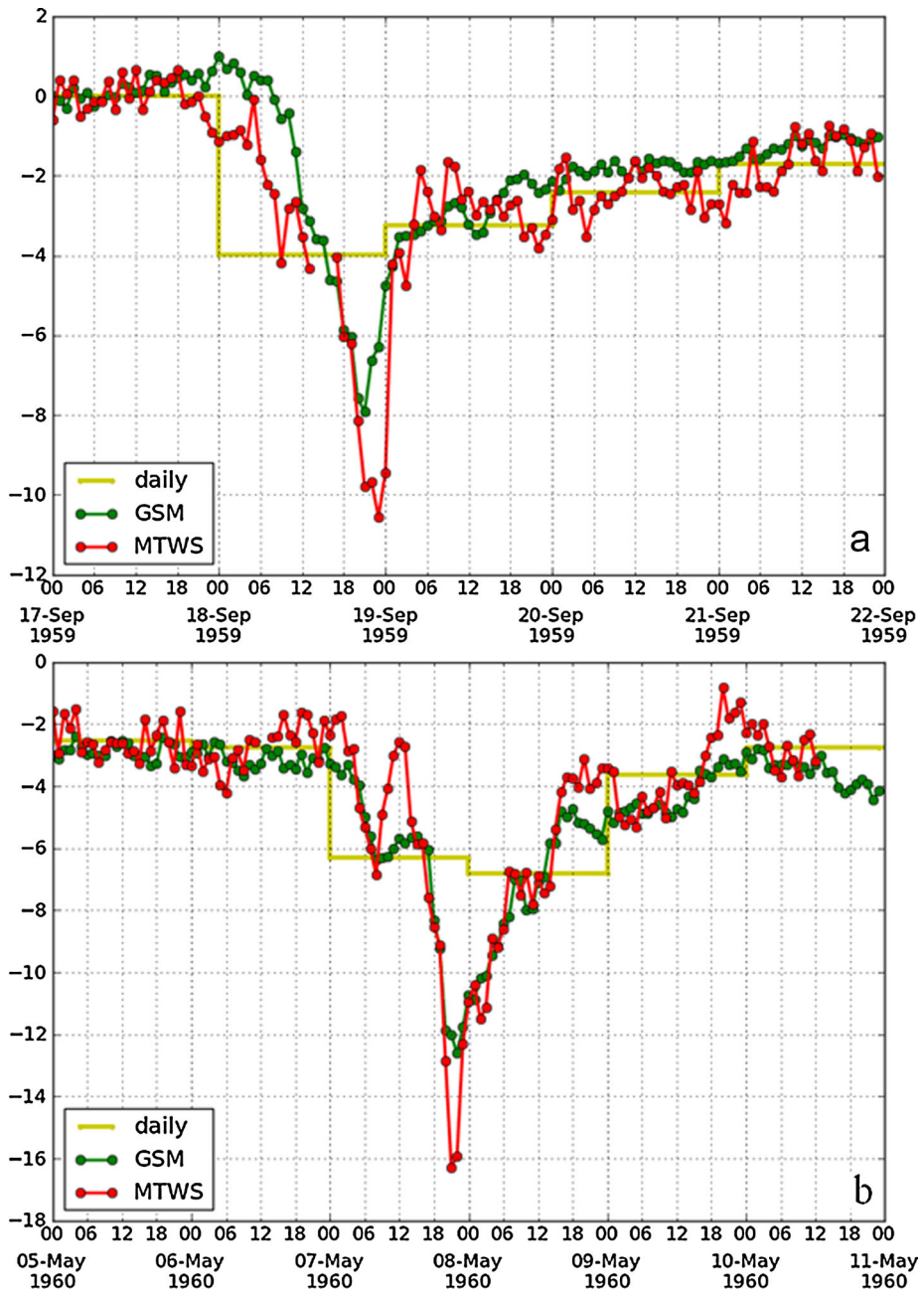
Figure 9 CR variations observed at the MTWS station and obtained through the GSM for the periods (**a**) 17 – 22.09.1957 and (**b**) 5 – 11.05.1960.
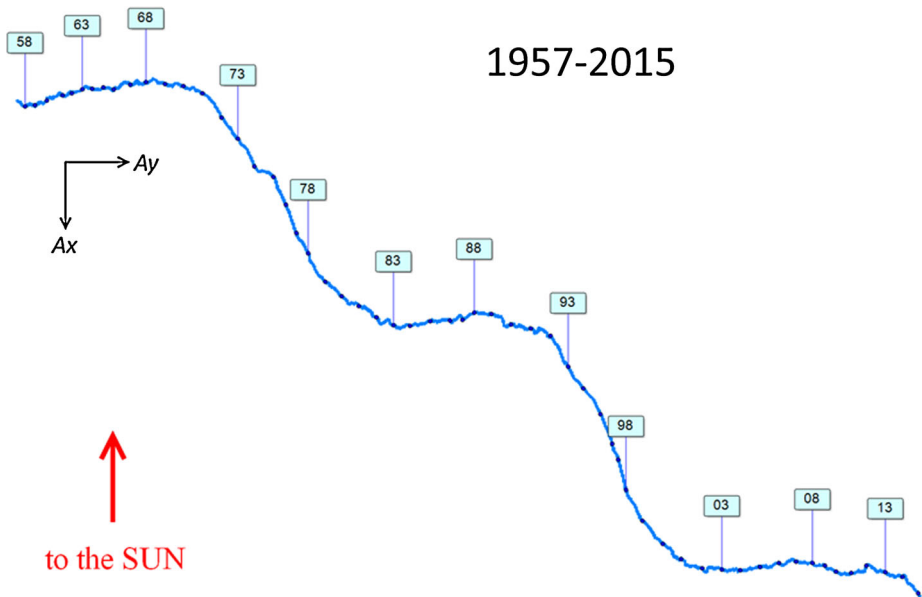
Figure 10 Vector diagram of the solar diurnal CR anisotropy for 1957 – 2015, obtained from hourly data of the NM network after processing with the GSM.

6. Some Results Obtained when the GSM Is Applied

The world-wide neutron monitor network (NMN) is an excellent tool for measuring the CR anisotropy, and most of our knowledge on the anisotropy has been obtained with its help. Figure 10 shows the "hooked" vectorgram from vectors of the equatorial component of the first harmonic of the CR anisotropy (or solar diurnal anisotropy) obtained for each hour within the past 58 years. Thus, about 500,000 vectors have been assembled and are presented in Figure 10. The long-term behavior of the CR anisotropy reflects the regular solar recurrence very well. The most apparent solar recurrence is the solar (22-year) magnetic cycle that controls the phase of the anisotropy. This relationship is so apparent that if only CR observations were used in order to estimate the existence of a magnetic cycle, they would be sufficient. Unlike the phase, the amplitude of the anisotropy is controlled by the 11-year cycle of solar activity (Belov, 2000). Figure 10 contains valuable data on long-term structural changes of the helio-magnetosphere and the spatial distribution of GCRs.

This rather regular picture depicted in Figure 10 changes dramatically at shorter timescales. The data of NMs showed that the anisotropy of galactic CRs sometimes (as a rule, during the arrival at Earth of large interplanetary disturbances) increased significantly, reaching 10% in separate shocks (Belov, 2008). During these periods, the CR anisotropy changes rapidly and strongly, which reflects the structures and dynamics of interplanetary disturbances. Thus, changes in the anisotropy determined by NM data provide the history of the solar wind, which is constantly supplemented and extended even to periods when direct measurements of the solar wind were not available (Belov, 2008; Asipenka *et al.*, 2009; Papaioannou *et al.*, 2010).

Forbush decreases (also known as FEs) are perhaps the most visible and variable phenomena in CR variations (Lockwood, 1971; Cane, 2000; Belov, 2008). They are caused either by solar coronal mass ejections (CMEs) or high-speed streams (HSS) of the solar
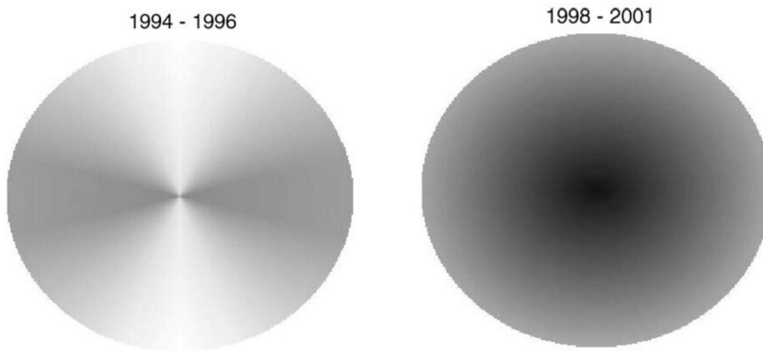
Figure 11 Distribution of protons with energy of > 2 GeV nucleon^{-1} calculated for the minimum and maximum solar activity in the sphere of 5 AU around the Sun based on data from *Ulysses* and the NM network. We see the distribution of the CR density in the heliosphere during the maximum (*right-hand side*) and minimum (*left-hand side*) of the solar activity. The *darker places* correspond to the lower CR density.

wind from coronal holes (CHs). NMs have provided, and continue to provide to this day, the main part of our information on FDs. In recent years, the IZMIRAN group created a database on FEs and interplanetary disturbances based on hourly data of the CR density and anisotropy calculated by means of the GSM. At present, this database includes more than 7000 events collected in the time interval from 1957 to 2016 (FEID, it can be openly accessed at spaceweather.izmiran.ru/eng/dbs.html).

During Solar Cycles 19 and 20, it was not possible to observe CMEs because there was no dedicated continuous mission for the purpose, and the observations were sometimes inaccurate later on. However, FEs provide the complete history of geoeffective emissions of the Sun. Other features of the FEs include i) changes in the CR density and the anisotropy during FDs (FEs) that reflect the structure of interplanetary disturbances (shock waves, borders of magnetic clouds, *etc.*); ii) changes in CR variations begin long before the arrival of the solar-wind disturbances at Earth and thus can be used to predict them; iii) FEs are, as a rule, observed simultaneously with geomagnetic and ionospheric disturbances and, hence, their observations can be used for geomagnetic and ionosphere forecasts; and iv) FD frequency and size reflect the changes imposed by the solar activity and can be used for the analysis and the forecast of bursts in the solar activity (Belov *et al.*, 2008). All of these advantages highlight the value of FEs and NM data, in particular.

Different types of CR measurements cannot simply replace each other, but they can complement each other very well: the more important and the more long-lived a space mission, the higher the need of ground-level support and the more frequent the need for data of the same NMs. The extremely successful flight of the *Ulysses* spacecraft (Wenzel *et al.*, 1992), which in many aspects provided the modern comprehensive understanding of the structure of the heliosphere and its cyclic changes, can serve as an example of such a mission.

In comparison with *Ulysses*, which flew in a wide range of helio-radii and helio-latitudes, one might say that Earth is fixed. The CR variations observed at Earth by NMs were therefore used to identify spatial and temporal variations in three periods of the *Ulysses* data (Belov *et al.*, 2003). The distribution of high-energy CRs in an internal heliosphere during periods of low (1994 – 1996) and high (1998 – 2001) solar activity (Figure 11) was one of the results of such a work. During solar-activity minimum the CRs density strongly depends on helio-longitude, and it almost does not depend on the distance from the Sun. In contrast,

during solar maximum, the latitudinal dependence decreases and the radial dependence becomes dominant.

It is interesting to note one of the consequences of the global reorganization of the heliosphere in which CRs participate. The size of the 11-year variation of CRs near the poles appears to be significantly higher than near the helio-equator, and, in particular, at Earth. It has been confirmed with data from *Ulysses* that in the second half of 2001 and in 2002, the spatial distribution of CRs in the internal heliosphere began to be reconstructed again. They were outside the simple symmetric shape and had perhaps partially restored a positive latitudinal gradient at high helio-latitudes.

Studying the index variations of geomagnetic activity as well as the CR density and anisotropy in high-speed streams of the solar wind from coronal holes showed that northern holes with negative polarity and southern holes with positive polarity are more effective than others in creating geomagnetic activity. The behavior of the CR anisotropy vector (especially its north–south component) depends heavily on the polarity of the magnetic field in the high-speed stream. These results have prediction potential and are therefore useful both for predicting geomagnetic activity and for diagnosing large-scale interplanetary disturbances that flow in the interplanetary medium.

7. Conclusions

We have presented the historical development, the scientific argumentation, and the mathematical formulation of the Global Survey Method (GSM), which combines data from all NMs that are distributed around the world.

The version of the GSM that has been developed in IZMIRAN and was described in this work has allowed us to obtain important characteristics of GCRs (density and anisotropy) outside the magnetosphere, using as input only the data of the world–wide network of NMs. The CR parameters were obtained for particles with a rigidity of 10 GV in each hour during the period of $1957 – 2016$ (> 60 years), which are unified in a dedicated database and are then combined in the database of "Forbush effects and interplanetary disturbances", together with the relevant parameters of the solar wind, the interplanetary environment, and solar and geomagnetic data. It allowed us to use the results of the GSM for the analysis of various manifestations of solar activity. The database that was implemented can also be further exploited by the scientific community and be the basis for the development and the improvement of various methods for predicting space weather, and in particular, for forecasting FEs and geomagnetic disturbances.

Although NM data and the GSM have been used extensively in recent years, this work combines all details, assumptions, and results in a comprehensive description. The validation of the method, its strengths and weaknesses, as well as possible future implementations and improvements were presented and discussed. Therefore, this article provides a clear statement of the method and gives all available insight so that the GSM can be reproduced and be further exploited by the scientific community.

References

Alania, M.V., Szabelski, J., Wawrzynczak, A.: 2003. In: Kajita, T., Asaoka, Y., Kawachi, A., Matsubara, Y., Sasaki, M. (eds.) *28th International Cosmic Ray Conference* **6**, 3585.

Aleksanyan, T., Bednazhevsky, V., Blokh, Y.L., Dorman, L., Starkov, F.: 1979. In: Miyake, S. (ed.) *16th International Cosmic Ray Conference* **4**, 315.

Altukhov, A.M., Krymsky, G.F., Kuzmin, A.I.: 1970, The method of "global survey" for investigating cosmic ray modulation. In: Somogyi, A., Nagy, E., Posch, M., Telbisz, F., Vesztergombi, G. (eds.) *11th International Conference on Cosmic Rays* **4**, 457.

Asipenka, A., Belov, A., Eroshenko, E., Klepach, E., Oleneva, V., Yanke, V.: 2009, *Adv. Space Res.* **43**(4), 708.

Belov, A., Baisultanova, L., Eroshenko, E., Mavromichalaki, H., Yanke, V., Pchelkin, V., Plainaki, C., Mariatos, G.: 2005, *J. Geophys. Res.* **110**(A9).

Belov, A., Abunin, A., Abunina, M., Eroshenko, E., Oleneva, V., Yanke, V., Papaioannou, A., Mavromichalaki, H., Gopalswamy, N., Yashiro, S.: 2014, *Solar Phys.* **289**(10), 3949. DOI.

Belov, A., Abunin, A., Abunina, M., Eroshenko, E., Oleneva, V., Yanke, V., Papaioannou, A., Mavromichalaki, H.: 2015, *Solar Phys.* **290**(5), 1429. DOI.

Belov, A.: 1980, Diss. Cand. Fiz.-mat. Sciences, IZMIRAN.

Belov, A.: 2000, *Space Sci. Rev.* **93**(1), 79.

Belov, A.: 2008, *Proc. Int. Astron. Union* **4**(S257), 439.

Belov, A., Eroshenko, E.: 1981. In: *International Cosmic Ray Conference* **4**, 97.

Belov, A., Blokh, Y.A., Dorman, L., Eroshenko, E., Inozemtseva, O., Kaminer, N.: 1973. In: *International Cosmic Ray Conference* **2**, 1247.

Belov, A., Blokh, I.L., Dorman, L., Eroshenko, E., Inozemtseva, O., Kaminer, N.: 1974, *Izv. Akad. Nauk SSSR, Ser. Fiz.* **38**, 1867.

Belov, A., Eroshenko, E., Heber, B., Yanke, V., Raviart, A., Müller-Mellin, R., Kunow, H.: 2003, *Ann. Geophys.* **21**, 1295.

Belov, A., Eroshenko, E., Oleneva, V., Yanke, V.: 2008, *J. Atmos. Solar-Terr. Phys.* **70**(2), 342.

Bieber, J., Evenson, P.: 1995. In: *International Cosmic Ray Conference* **4**, 1316.

Cane, H.V.: 2000, *Space Sci. Rev.* **93**(1), 55.

Chirkov, N.P., Altukhov, A.I., Krymsky, G.F., Krivoshapkin, P.A., Kuzmin, A.I., Skripin, G.V.: 1967, *Geomagn. Aeron.* **7**, 621.

Clem, J.M., Dorman, L.I.: 2000, *Space Sci. Rev.* **93**(1), 335.

Dorman, L.: 1972, *Meteorological Effects of Cosmic Rays*, Nauka, Moscow, 211 p.

Dorman, L., Yanke, V.: 1971a, *Izv. Akad. Nauk SSSR, Ser. Fiz.* **35**(12), 2556.

Dorman, L., Yanke, V.: 1971b, *Izv. Akad. Nauk SSSR, Ser. Fiz.* **35**(12), 2571.

Dorman, L.I., Smirnov, V.S., Tyasto, M.: 1971, *Cosmic Rays in the Earth's Magnetic Field*, Nauka, Moscow, 400 p.

Dorman, L.: 1957, *Variations of Cosmic Rays*, Gosteichteorizdat, Moscow.

Dorman, L.: 2009, *Cosmic Rays in Magnetospheres of the Earth and Other Planets* **358**, Springer, Dordrecht. DOI.

Dorman, L.: 2013, *Cosmic Rays in the Earth's Atmosphere and Underground* **303**, Springer, Netherlands. DOI.

Dorman, L., Fedchenko, S., Granitsky, L., Rishe, G.: 1970. In: *International Cosmic Ray Conference* **2**, 233.

Dvornikov, V., Kravtsova, M., Sdobnov, V.: 2006, *Bull. Russ. Acad. Sci., Phys.* **70**(10), 1504.

Dvornikov, V., Sdobnov, V., Sergeev, A.: 1983. In: *International Cosmic Ray Conference* **3**, 249.

Forsythe, J., Malcolm, M., Mouler, K.: 1980, *Numerical Methods of Mathematical Calculations*, Mir, Moscow.

Jung, J., Oh, S., Yi, Y., Evenson, P., Pyle, R., Jee, G., Kim, J.-H., Lee, C., Sohn, J.: 2016, *J. Astron. Space Sci.* **33**(4), 345.

Kobelev, P., Belov, A., Eroshenko, E., Yanke, V.: 2013. In: *Proc. 33rd ICRC*, *Rio de Janeiro*.

Korotkov, V., Berkova, M., Belov, A., Eroshenko, E., Yanke, V., Pyle, R.: 2013, *J. Geophys. Res.* **118**(11), 6852.

Korotkov, V., Berkova, M., Belov, A., Eroshenko, E., Kobelev, P., Yanke, V.: 2011, *Geomagn. Aeron.* **51**(2), 247. DOI.

Krymsky, G.F., Kuzmin, A.I., Chirkov, N.P., Krivoshapkin, P.A., Skripin, G.V.: 1966a, *Geomagn. Aeron.* **6**(8), 991.

Krymsky, G.F., Altukhov, A.M., Kuzmin, A.I., Skripin, G.V.: 1966b, *A New Method for Studying the Anisotropy of Cosmic Rays – Investigation of Geomagnetism and Aeronomy*, Nauka, Moscow, 105

Krymsky, G.F., Kuzmin, A.I., Krivoshapkin, P.A., Samsonov, I.S., Skripin, G.V., Transkii, I.A., Chirkov, N.P.: 1981, *Cosmic Rays and Solar Wind*, Nauka, Novosibirsk.

Lockwood, J.: 1990, *Solar-Geophys. Data* **549**, 154.

Lockwood, J.A.: 1971, *Space Sci. Rev.* **12**(5), 658.

Lukovnikova, A.: 2012, Diss. Cand. Fiz.-mat. Sciences, Irkutsk.

McCracken, K., Rao, U., Shea, M.: 1962, *The Trajectories of Cosmic Rays in a High Degree Simulation of the Geomagnetic Field* **77**, Massachusetts Inst. of Tech., Lab. for Nuclear Science, Cambridge.

McCracken, K., Rao, U., Fowler, B., Shea, M., Smart, D.: 1965, IQSY Instruction Manual No. 10, IQSY Committee, Washington.

Moraal, H., Belov, A., Clem, J.: 2000, *Space Sci. Rev.* **93**(1), 285.

Nagashima, K.: 1971, *Rep. Ionos. Space Res. Jpn.* **25**, 189.

Nagashima, K., Sakakibara, S., Murakami, K., Morishita, I.: 1989, *Nuovo Cimento C* **12**(2), 173.

Papailiou, M., Mavromichalaki, H., Belov, A., Eroshenko, E., Yanke, V.: 2012a, *Solar Phys.* **280**(2), 641. DOI.

Papailiou, M., Mavromichalaki, H., Belov, A., Eroshenko, E., Yanke, V.: 2012b, *Solar Phys.* **276**(1), 337. DOI.

Papailiou, M., Mavromichalaki, H., Abunina, M., Belov, A., Eroshenko, E., Yanke, V., Kryakunova, O.: 2013, *Solar Phys.* **283**(2), 557. DOI.

Papaioannou, A., Mavromichalaki, H., Eroshenko, E., Belov, A., Oleneva, V.: 2009a, *Ann. Geophys.* **27**, 1019. DOI.

Papaioannou, A., Belov, A., Mavromichalaki, H., Eroshenko, E., Oleneva, V.: 2009b, *Adv. Space Res.* **43**(4), 582. DOI.

Papaioannou, A., Malandraki, O., Belov, A., Skoug, R., Mavromichalaki, H., Eroshenko, E., Abunin, A., Lepri, S.: 2010, *Solar Phys.* **266**(1), 181. DOI.

Pomerantz, M., Duggal, S.: 1972, *J. Geophys. Res.* **77**(1), 263.

Richardson, I., Dvornikov, V., Sdobnov, V., Cane, H.: 2000, *J. Geophys. Res.* **105**(A6), 12579. DOI.

Sergeev, A.V.: 1974, Diss. Cand. Fiz.-mat. Sciences, Research Institute of Nuclear Physics of the Moscow State University.

Shea, M.A., Smart, D.F., McCall, J.R.: 1968, *Can. J. Phys.* **46**(10), S1098. DOI.

Shea, M.A., Smart, D.F., McCracken, K.G., Rao, U.R.: 1968, *Supplement to IQSY Instruction Manual No. 10 Cosmic Ray Tables: Asymptotic Directions, Variational Coefficients and Cutoff Rigidities*, Air Force Cambridge Research Labs LG Hanscom Field Mass.

Shea, M.A., Smart, D.F., Humble, J.E., Fluckiger, E.O., Gentile, L.C., Humble, J.E., Nichol, M., Shea, M.A., Smart, D.F.: 1987. In: Kozyarivsky, V.A., Lidvansky, A.S., Tulupova, T.I., Tayabuk, A.L., Voevodsky, A.V., Volgemut, N.S. (eds.) *Proc. 20th Int. Cosmic Rays Conf.* **3**, Nauka, Moscow, 171.

Simpson, J.A.: 2000, The cosmic ray nucleonic component: the invention and scientific uses of the neutron monitor. *Space Sci. Rev.* **93**, 11. DOI. Cosmic Rays and Earth, Springer

Smart, D.F.: 1997. In: Potgieter, M.S., Raubenheimer, B.C., van der Walt, D.J. (eds.) *25th International Cosmic Ray Conference* **2**, 401.

Wenzel, K., Marsden, R., Page, D., Smith, E.: 1992, *Astron. Astrophys. Suppl. Ser.* **92**, 207.

Yasue, S., Mori, S., Sakakibara, S., Nagashima, K.: 1982, Report of Cosmic-Ray Research Laboratory, Nagoya, 7.